Spin effects in exclusive ρ^0 meson production at COMPASS experiment*

O.A. Grajek

On behalf of the COMPASS Collaboration

HEP Division, A. Soltan Institute for Nuclear Studies (SINS),
ul. Hoża 69, PL-00-681 Warsaw, Poland

Preliminary results from exclusive production of ρ^0 mesons at the COMPASS experiment at CERN, using a 160 GeV polarized muon beam and a large polarized nuclear target, are presented. The studied reaction is exclusive *incoherent* ρ^0 production, $\mu N \to \mu N \rho^0$, with N being the nucleon in any of the nuclei of the target. The measurements were done in a wide range of Q^2: $0.01 < Q^2 < 10$ GeV^2, at $\langle W \rangle \approx 10$ GeV. The results for r^{04}_{00}, $r^{1}_{1\,-1}$, $r^{04}_{1\,-1}$ and $\mathrm{Im}\, r^{3}_{1\,-1}$ ρ^0 spin density matrix elements and the ratio $R = \sigma_L/\sigma_T$, based on 700 000 events selected from 2002 data, are shown and commented.

PACS numbers: 13.60.Le, 14.40.Cs, 13.88.+e

1. Introduction

1.1. The reaction under study

The COMPASS experiment at CERN has two programs — one using a polarized muon beam and another with hadron beams, called muon and hadron program, respectively. One of the subjects of the muon program are studies of exclusive muoproduction of vector mesons (VM). Here we present results of the analysis of exclusive *incoherent* ρ^0 mesons production, based on COMPASS 2002 data.

The investigated reaction is

$$\mu \, + \, N \, \to \, \mu \, + \, N + \, \rho^0 \, . \tag{1}$$

It can be alternatively described as the reaction

$$\gamma^* \, + \, N \, \to \, \rho^0 \, + \, N \, , \tag{2}$$

* Presented at the *Cracow Epiphany Conference on Hadron Spectroscopy*, Cracow, 6–8 January, 2005.

Table I. Kinematical variables describing reactions (1) and (2).

Symbol	Meaning
$k = (E,\, \mathbf{k})$	4-momentum of the incoming lepton
$k' = (E',\, \mathbf{k}')$	4-momentum of the scattered lepton
$p = (M,\, \mathbf{0})$	4-momentum of the target nucleon
$p' = (M,\, \mathbf{p}')$	4-momentum of the recoiled nucleon
$q = k - k' = (\nu,\, \mathbf{q})$	4-momentum of the virtual photon γ^*
v	4-momentum of the vector meson V
$Q^2 = -q^2$	virtuality of γ^*
$\nu = p \cdot q / M = E - E'$	energy of γ^* in the LAB frame
$W^2 = (q + p)^2$	squared total energy in the γ^*–N system
$t = (q - v)^2 = (p - p')^2$	squared 4-mom. transfer between γ^* and V
p_t^2	squared transverse momentum of V w.r.t. γ^*
$M_X^2 = (p + q - v)^2$	squared mass of the recoiled hadron system
$E_{\rm miss} = (M_X^2 - M^2) \,/\, 2M$	measure of event exclusivity

with a subsequent ρ^0 decay into $\pi^+\pi^-$ pair. The virtual photons γ^* are emitted by muons, when the latter are scattered off the target nucleons. In reactions (1) and (2) N is the quasi-free nucleon in any of the nuclei of the COMPASS nuclear target. In Table I we present kinematical variables used to describe processes (1) and (2). We use the units in which $\hbar = c = 1$.

1.2. The physical picture of the studied reaction

Two theoretical approaches are being used to describe the reaction (2) — one based on the vector meson dominance (VMD) language, e.g. [2, 3], and the second based on the partonic language, e.g. [4, 5]. The former is applicable in a Q^2 range from photoproduction up to the values of the order of $10 \div 20$ GeV^2, so its particular merit is that it can describe the reaction (2) in the nonperturbative domain. The latter is to be used in a Q^2 range where perturbative quantum chromodynamics (pQCD) is applicable — above Q^2 of the order of 5 GeV^2.

The basic physical ideas behind the two mentioned approaches are quite similar. The virtual photon γ^* fluctuates into a virtual VM (VMD picture) or $q\bar{q}$ pair (partonic picture). Therefore the reaction (2) allows to study the *hadron structure* of the virtual photon, see e.g. [2]. This virtual state is transformed into the real VM in the final state via the interaction with

the nucleon. This interaction is mediated by an object exchanged in the t-channel of the process (2).

In the VMD picture this object is called reggeon. If the energy W of the reaction (2) is high enough (several tens GeV) — the dominant exchanged reggeon is *pomeron*. At lower W pomeron also participates, but the exchanges of other reggeons, with intercepts of their trajectories lower than 1 and appropriate quantum numbers, predominate. In the VMD picture one is not concerned with the internal structure of the reggeons and target nucleon, or, more precisely, in the constituents these objects are possibly made of. A thorough presentation of the VMD approach and what can be learned using it to describe the process (2) can be found in [2].

In the partonic picture one is interested in the constituents of which the reggeons and target nucleon are made of, and tries to describe the process (2) in terms of these constituents. Here pomeron is modelled as a pair of gluons, whereas other reggeons are introduced as t-channel $q\bar{q}$ pairs. As the process (2) is exclusive one, the internal structure of the nucleon has to be described in terms of the *generalized parton distributions* (GPDs), see e.g. [6]. They are generalizations of the "ordinary" parton distributions, introduced to describe inclusive lepton–nucleon scattering. Application of GPDs to the reaction (2) can be found in [7]. Since the experimental information concerning GPDs is still limited, the possible access to GPDs via exclusive ρ^0 production is one of reasons why we are studing this process at COMPASS.

As the reaction (2) occurs predominantly with $|t|$ lower than $\sim$1 GeV^2, it shows features characteristic for *diffractive* hadron processes, namely a pronounced forward peak in the t distribution, and a weak dependence on W. Therefore it is often called diffractive VM production.

For a review of both mentioned theoretical approaches and of the experimental situation see [8] and references therein.

1.3. Angular distributions of the ρ^0 meson production and decay

In this analysis we are interested in the spin effects in exclusive incoherent ρ^0 meson production. They are evaluated using the elements of the ρ^0 spin density matrix. These elements parametrize the angular distribution of ρ^0 meson production and decay [9, 2].

In general, the angular distribution of VM production and decay is a 3-dimensional function of 3 angles θ, ϕ and Φ, $\mathcal{W} = \mathcal{W}(\cos\theta,\ \phi,\ \Phi)$ [9, 2]. To define the angle Φ one has to perform a Lorentz boost from the laboratory frame, where energies and 3-momenta of detected particles are determined, to the γ^*–N center-of-mass frame. Φ is an angle between the lepton scattering plane, defined by 3-momenta of incoming and scattered

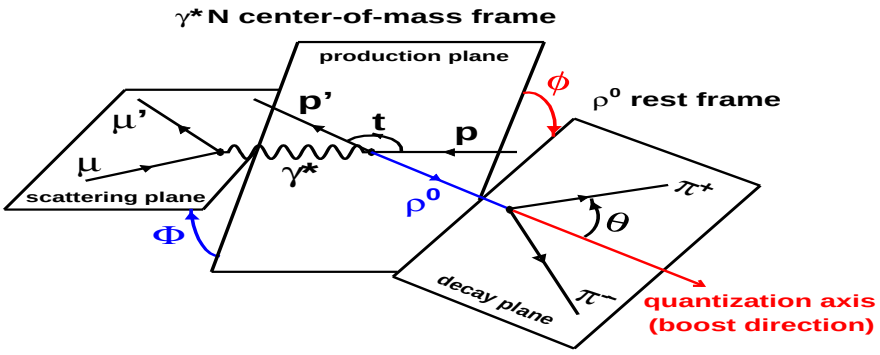

Fig. 1. Angles and planes used to describe exclusive ρ^0 production and decay.

lepton, and the VM production plane, defined by 3-momenta of parent γ^* and produced VM. To define the angles θ and ϕ, the next Lorentz boost is needed, from the γ^*–N center-of-mass frame to the VM rest frame. The latter is defined as a frame in which the sum of 3-momenta of the particles from a 2-body VM decay is zero. In this frame the angles θ and ϕ are defined in the *s-channel helicity system*, in which the direction of both Lorentz boosts is taken as the quantization axis. θ is the polar, and ϕ the azimuthal angle of the positively charged particle from a 2-body VM decay. ϕ is also an angle between the VM production and VM decay planes. All the angles, planes and frames are shown in Fig. 1.

If the hypothesis of s-channel helicity conservation holds, the angular distribution $\mathcal{W}$ depends solely on the difference of Φ and ϕ angles. Therefore one introduces the angle $\psi = \phi - \Phi$, and writes $\mathcal{W} = \mathcal{W}(\cos\theta,\ \psi)$.

In this analysis we study 1-dimensional projections $\mathcal{W}(\cos\theta)$, $\mathcal{W}(\phi)$, $\mathcal{W}(\Phi)$ and $\mathcal{W}(\psi)$ of the angular distribution. Each of these projections is obtained after integrating $\mathcal{W}(\cos\theta,\ \phi,\ \Phi)$ or $\mathcal{W}(\cos\theta,\ \phi)$ over remaining angles. Such approach gives an access to 4 individual VM spin density matrix elements and 3 linear combinations of 6 other ones. The analysis of $\mathcal{W}(\cos\theta,\ \phi,\ \Phi)$ is planned after including 2003 and 2004 data.

1.4. Spin density matrix of the ρ^0 meson

The ρ^0 spin density matrix (SDM) elements allow to study the helicity structure of the reaction (2), as they are linear combinations of the helicity amplitudes $T_{\lambda_2\lambda_1}$ describing (2). Here λ_1 and λ_2 stand for helicities of γ^* and VM, respectively (λ_1 or $\lambda_2 = -1,\ 0,\ 1$), while helicities of the target and recoiling nucleon are summed up. We use the formalism presented in [9], which applies to the case of an unpolarized target. How we apply it to

our polarized target is explained in Sec. 4.

One of the issues we study is the s-channel helicity conservation (SCHC) hypothesis. SCHC hypothesis states that the vector meson retains the helicity of its parent virtual photon. If SCHC holds, one of the SDM elements can be used to determine the ratio $R = \sigma_L/\sigma_T$, where σ_L (σ_T) is the cross section for exclusive incoherent production of ρ^0 by longitudinally (transversely) polarized virtual photons (see Sec. 4 for details). The ratio R is an important parameter because it is directly related to the dynamics of exclusive VM production, and it provides a sensitive test for the models trying to describe this process.

SDM of ρ^0 meson contains 23 elements (for definitions see [9]). 15 of them can be determined experimentally using an unpolarized lepton beam, for accessing the remaining 8 ones a polarized lepton beam is necessary.

The most extensive and precise results concerning ρ^0 SDM elements were obtained by the high energy experiments ZEUS and H1 at DESY. However, as they use an unpolarized lepton beam they had no access to the 8 SDM elements. The E665 experiment at Fermilab, which finished its operation, with $\langle W \rangle$ roughly 2 times larger than that of COMPASS, and which also used a polarized muon beam, published results for 4 SDM elemets, one of them being that accessible with a polarized lepton beam. The HERMES experiment at DESY and the experiments at the Jefferson Lab have polarized lepton beams and can access all 23 SDM elements, however, all these experiments operate at low energies. The COMPASS experiment using a polarized muon beam can determine all 23 SDM elements in the moderate W range with high precision.

The trigger system at COMPASS allows to cover an extended Q^2 range $\sim 5 \times 10^{-4} < Q^2 < \sim 25$ GeV^2 for the process of interest. With the 2002 data alone, for which a limited subrange $0.01 < Q^2 < 10$ GeV^2 was studied, we extended the investigated Q^2 domain by an order of magnitude down with respect to all mentioned experiments, and significantly improved the statistical precision (see Sec. 4).

2. The COMPASS experimental setup

A brief description of the COMPASS experimental setup is given here. A more thorough presentation can be found in [1, 10] and references therein, which concern particular detectors and software.

The COMPASS (NA-58) experiment is set up at the M2 muon beamline at CERN. The beam delivered to COMPASS, consisting of positively charged muons, has a mean energy of 160 GeV, mean polarization with respect to the beam direction -0.76, and an intensity of 2×10^8 muons/spill of a length of 4.8 s and a cycle-time of 16.8 s.

Our polarized target consists of 2 cylindrical cells of a length of 60 cm and a diameter of 3 cm each, separated by a gap of 10 cm long. Both cells are filled with ^{6}LiD, used as the deuteron target material. The cells are placed within a superconducting solenoid magnet, producing a highly homogeneous magnetic field of 2.5 T directed along z (longitudinal) target axis. In addition a dipole magnet is installed, which allows to reverse the polarizations of both cells. The cells are contained in a large cryogenic system, using a mixture of ^{3}He/^{4}He as a cooling medium. The ^{6}LiD target material is longitudinally polarized via dynamic nuclear polarization (see e.g. [1]), which allows to get polarizations of the order of $0.50 \div 0.55$. During data taking both target cells are polarized in opposite directions, and their polarizations are reversed every 8 hours.

The COMPASS experimental setup is a one-arm spectrometer more than 50 m long. It has been designed to detect the scattered muons and the produced hadrons in wide momentum and angular ranges. To achieve this the spectrometer is subdivided into two stages, called Large Angle Spectrometer (LAS) and Small Angle Spectrometer (SAS). Both LAS and SAS are based on large dipole magnets — SM1 and SM2, respectively. SM1 is a large aperture magnet, accepting particles with momenta larger than 0.4 GeV, while SM2 accepts particles with momenta larger than 4 GeV. LAS and SAS are equipped with diverse tracking detectors, hadron calorimeters, and muon identification devices.

At COMPASS several detectors based on new technologies are used. Particularly MicroMeGas and GEM trackers are installed in a region close to a beam due to a high beam intensity. A beam area downstream of the target is covered by scintillating fibre detectors. Moderate and large angle tracking is provided by drift chambers, multiwire proportional chambers and large straw chambers. The identification of the scattered muons is performed by two muon wall detectors, placed behind hadron absorbers. Hadron–lepton separation and hadron energy measurements are provided by two large iron-scintillator sampling calorimeters. LAS is also equipped with a large gaseous RICH detector for particle identification, but an information from RICH is not used in the present analysis.

The trigger is based on detection of the scattered muons by the scintillator hodoscope planes. The muon trigger is subdivided into several subsystems, allowing to cover a very broad Q^2 range from $\sim 5 \times 10^{-4}$ up to ~ 100 GeV^2. In addition signals from hadron calorimeters are used for triggering. Several veto counters installed upstream of the target are used to reject false triggers caused by the beam halo and pile-up muons.

3. Data sample

The results presented here have been obtained in the analysis of 2002 data taken with the longitudinally polarized target.

As mentioned in Sec. 1.4, we parametrize the angular distributions with the formulae, which are applicable in a case of an unpolarized target. Therefore we combine events from both target cells. The necessary elements to get the net target polarization close to zero are the target spin reversals and approximately the same amounts of data taken with both target-spin configurations. It has been checked that in the present analysis the mean target polarization is very close to zero.

For an event to be accepted as exclusive ρ^0 production, the presence of the reconstructed primary vertex, with the associated incoming and scattered muon tracks, was required. The vertex should contain only 2 additional outgoing hadron tracks with opposite charges. The vertex had to be contained in one of the target cells.

The following cuts have been applied to the kinematical variables: $Q^2 > 0.01$ GeV^2, $E_{\mu\prime} > 20$ GeV, and $\nu > 30$ GeV. These cuts were imposed to avoid large corrections for acceptance, kinematical smearing and misidentifications of events.

As mentioned in Sect. 2, the particle identification by RICH was not required, because interesting events could be selected using the distribution of the invariant mass of ρ^0 decay produts. For that, two mass hypotheses were assigned to both hadron tracks, namely masses of charged pions and kaons, and $m_{\pi\pi}$ and m_{KK} invariant masses were calculated. The $m_{\pi\pi}$ distribution for the finally selected exclusive sample (without cuts on $m_{\pi\pi}$) is shown in Fig. 2 (top panel). A clear ρ^0 peak centered around 770 MeV can be seen. It is slightly skewed towards smaller values, which is due to the interference of the amplitudes describing the reaction (2) and the non-resonant s-wave $\pi^+\pi^-$ pairs production, known as Drell process [11], which constitutes the non-resonant background. One can see (right to the ρ^0 peak) that this background is at a very low level compared to the signal. Preliminary studies of the $m_{\pi\pi}$ distribution have been performed and it has been found [12] that the observed skewing can be well described in the whole selected Q^2 range by the Söding model [13]. As a small amount of K^+K^- pairs coming from ϕ mesons decays is present in the exclusive sample without cuts on $m_{\pi\pi}$, a bump around 0.4 GeV appears. It is due to assignment of the pion mass to the kaon tracks. To reject the non-resonant background outside of the ρ^0 peak and to get rid of the K^+K^- pairs, cuts $0.5 < m_{\pi\pi} < 1$ GeV (marked with arrows in Fig. 2) have been imposed.

At COMPASS the recoiling hadrons with low momenta are not detected. To select the exclusive ρ^0 production events, $E_{\rm miss}$ was used as a measure

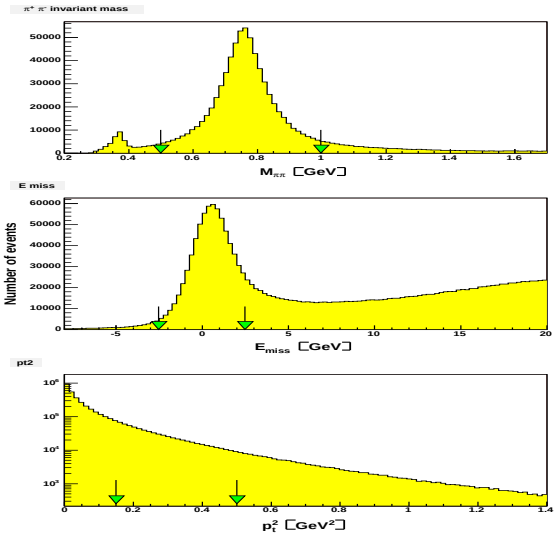

Fig. 2. Experimental distributions of $m_{\pi\pi}$ (top panel), $E_{\rm miss}$ (middle panel) and p_t^2 (bottom panel). See text for details.

of event exclusivity. The distribution of $E_{\rm miss}$ for the final exclusive sample (without cuts on $E_{\rm miss}$) is shown in Fig. 2 (middle panel). For the exclusive event $M_X^2 = M^2$, therefore $E_{\rm miss}$ distribution should be peaked around 0. A clear exclusive peak can be noticed in Fig. 2. Its width is determined by the spectrometer resolution. A part of the distribution right to the exclusive peak is due to non-exclusive events: double-diffractive ρ^0 production accompanied with the dissociation of the nucleon, which decay products remain undetected, and semi-inclusive ρ^0 production, with other particles escaping detection. To select exclusive events the cut $|E_{\rm miss}| < 2.5$ GeV (marked with arrows in Fig. 2) has been imposed. An amount of the non-exclusive background in the selected exclusive sample has been estimated to be of the order of $10 \div 15\%$. Further studies of this background are under way.

Finally cuts on p_t^2 were applied: $0.15 < p_t^2 < 0.5$ GeV^2. The p_t^2 distribution for the final exclusive sample (without cuts on p_t^2) is shown in Fig. 2 (bottom panel). The cuts are marked with arrows. The lower cut rejects events of exclusive coherent ρ^0 production, i.e. production on any of the COMPASS target nuclei which recoils intact. The upper cut is to further suppress contribution of the non-exclusive background.

Radiative corrections have been neglected in the present analysis. They are expected to be small, particularly due to the requirement of events exclusivity via the $E_{\rm miss}$ cut.

After all selections **695 500** events of exclusive incoherent ρ^0 production have been obtained. They were divided into 5 bins in Q^2, which limits and $\langle Q^2 \rangle$ values and numbers of events within them are given in Tab. II. For the final sample $\langle W \rangle = 10.4$ GeV, and $\langle p_t^2 \rangle = 0.23$ GeV^2.

Table II. Characteristics of the sample used in the present analysis

Bin of Q^2	1	2	3	4	5
Q^2 range [GeV^2]	0.01 ÷ 0.05	0.05 ÷ 0.3	0.3 ÷ 0.6	0.6 ÷ 2.0	> 2.0
$\langle\, Q^2 \,\rangle$ [GeV^2]	0.025	0.128	0.416	1.01	3.30
No. of events	306 k	293 k	56 k	35 k	6 k

4. Results

Fig. 3 shows the 1-dimensional angular distributions of $\cos\theta$, ϕ, Φ, and ψ angles, in 5 bins of Q^2. The angular distributions determined experimentally were corrected for acceptance, reconstruction efficiency, and kinematical smearing effects. These effects were determined on a basis of Monte Carlo data with complete spectrometer simulation and reconstruction of events.

Theoretically predicted distributions, obtained after intergrating formulae (92) and (92a) for $\mathcal{W}(\cos\theta,\ \phi,\ \Phi)$ given in [9], are the following:

$$W(\cos\theta) \;=\; \frac{3}{4}\,[\,(1 \,-\, \underline{r^{04}_{00}}) \,+\, (3\,\underline{r^{04}_{00}} \,-\, 1)\,\cos^2\theta\,]\,, \tag{3}$$

$$W(\phi) \;=\; \frac{1}{2\pi}\,(1 \,-\, 2\,\underline{r^{04}_{1\,-1}}\,\cos 2\phi \,+\, 2\,P_{\rm b}\,\sqrt{1-\epsilon^2}\,\underline{\mathrm{Im}\,r^{3}_{1\,-1}}\,\sin 2\phi)\,, \tag{4}$$

$$\begin{aligned} W(\Phi) \;=\; \frac{1}{2\pi}\,[\,1 \,-\, (\underline{2\,r^{1}_{11} \,+\, r^{1}_{00}})\,\epsilon\,\cos 2\Phi \\ + (\underline{2\,r^{5}_{11} \,+\, r^{5}_{00}})\,\sqrt{2\epsilon\,(1\,+\,\epsilon)}\,\cos\Phi \\ + (\underline{2\,r^{8}_{11} \,+\, r^{8}_{00}})\,P_{\rm b}\,\sqrt{2\epsilon\,(1\,-\,\epsilon)}\,\sin\Phi\,]\,, \end{aligned} \tag{5}$$

$$W(\psi) \;=\; \frac{1}{2\pi}\,(1 \,+\, 2\,\epsilon\,\underline{r^{1}_{1\,-1}}\,\cos 2\psi)\,, \tag{6}$$

with r^{04}_{ij} and r^{α}_{jk} being the SDM elements (underlined for better visibility; see [9] for definitions), $P_{\rm b}$ being beam polarization, and ϵ denoting virtual photon polarization parameter. ϵ is related to the ratio Γ_L/Γ_T of fluxes of the longitudinally and transversely polarized virtual photons (denoted as γ^*_L and γ^*_T in what follows) via $\epsilon + \delta = \Gamma_L/\Gamma_T$, where δ is the correction

factor taking into account the non-zero lepton projectile mass [9]. The element $\mathrm{Im}\, r^3_{1\,-1}$ in Eq. (4) and the combination $2r^8_{11} + r^8_{00}$ in Eq. (5) are only accessible by experiments with polarized lepton beams, as they enter mentioned formulae multiplied by P_b. Prior to COMPASS only $\mathrm{Im}\, r^3_{1\,-1}$ element has been determined at moderate W, by the E665 experiment [14].

It should be mentioned, that formula (6) is valid only if SCHC holds, whereas formulae (3)–(5) are general.

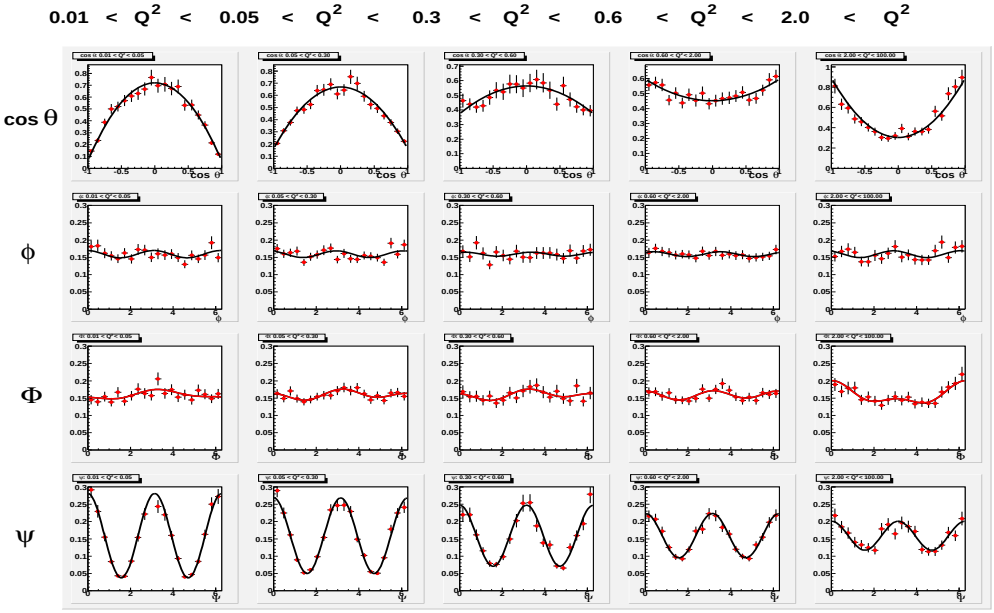

Fig. 3. The distributions $\mathcal{W}(\cos\theta)$, $\mathcal{W}(\phi)$, $\mathcal{W}(\Phi)$ and $\mathcal{W}(\psi)$ in 5 bins of Q^2 (shown at the top of the figure). Experimental results are shown with dots, vertical bars represent the statistical errors alone, longitudinal bars show angular bins. Solid curves are results of the fits discussed in a text.

These formulae, with the SDM elements as free parameters, were fitted to the experimental distributions, and the results of fits are shown in Fig. 3 as solid lines.

A change of behaviour of the $\cos\theta$ distribution with increase of Q^2, from $\sin^2\theta$–like to $\cos^2\theta$–like, is clearly visible. This is associated with an increasing amount of longitudinally polarized ρ^0 mesons in the sample. Also a pronounced decrease of the amplitude of oscillations of the ψ distributions is seen. These oscillations are produced only by the γ^*_T, and a contribution of such photons to the reaction (2) decreases with increase of Q^2. Both ϕ and Φ distributions are approximately flat (they should be constant if

SCHC holds).

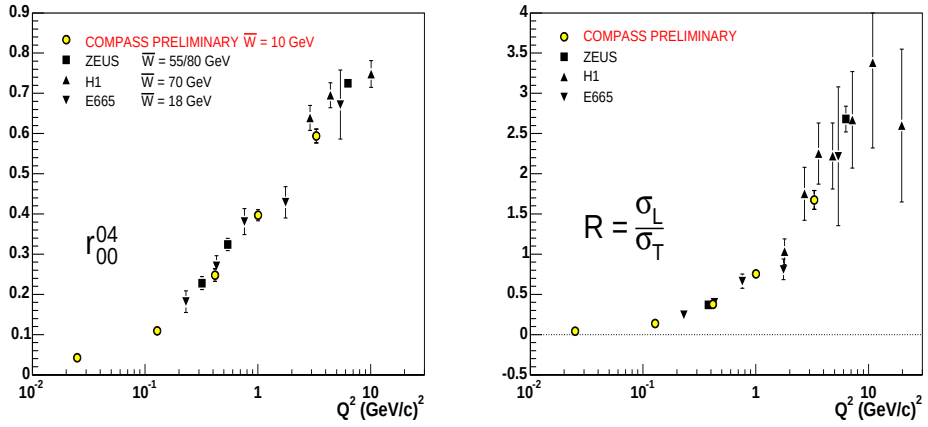

Fig. 4. r^{04}_{00} SDM element (left) and the ratio R (right) as functions of Q^2.

Now, let us discuss the SDM elements r^{04}_{00}, r^{1}_{1-1}, r^{04}_{1-1} and $\mathrm{Im}\, r^{3}_{1-1}$, obtained from fits to the angular distributions. These elements are shown as functions of Q^2 in Figs. 4 and 5, togehter with results from the ZEUS [15], H1 [16], and E665 [14] experiments.

For all 4 SDM elements one can see a good agreement of our results with those of other experiments. Our statistical uncertainties are comparable to those of ZEUS, and significantly smaller than those of H1 and E665. As mentioned above, we extend the studied Q^2 range by an order of magnitude down with respect to all others experiments.

The SDM element r^{04}_{00} has a direct physical interpretation as a fraction of *longitudinally* polarized ρ^0 mesons in a sample. It is observed that it increases with increase of Q^2.

If SCHC holds, one can use the r^{04}_{00} SDM element to obtain the ratio $R = \sigma_L/\sigma_T$. These two quantities are related via

$$R \;=\; \frac{1}{\epsilon+\delta}\,\frac{r^{04}_{00}}{1\;-\;r^{04}_{00}}\,. \qquad (7)$$

The ratio R is presented as a function of Q^2 in Fig. 4 (right panel). Like for the SDM elements, one can see a good agreement of our results with those of other experiments. In our lowest Q^2 bin R is very close to zero. It can be explained as associated with approaching the photoproduction limit, where ρ^0 mesons are produced by real photons. Such photons can be only transversely polarized, and if SCHC holds, only transversely polarized ρ^0 mesons should be produced. Our R at lowest Q^2 agrees with the ZEUS

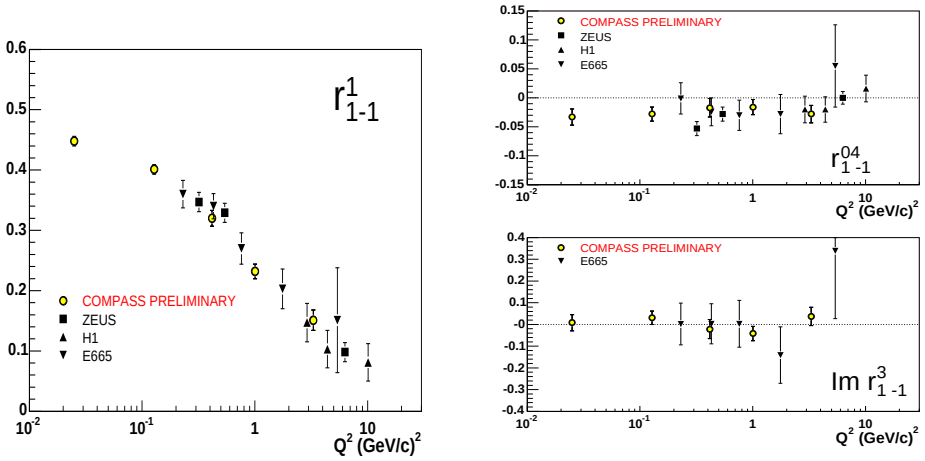

Fig. 5. $r^1_{1\,-1}$ (left) and $r^{04}_{1\,-1}$ and $\mathrm{Im}\, r^3_{1\,-1}$ (right) SDM elements as functions of Q^2.

result obtained from their quasi-photoproduction data [17] (not shown in Fig. 4). In [17] r^{04}_{00} has been determined to be consistent with zero, and $R = 0.06 \pm 0.03$. As Q^2 grows, ρ^0 production by γ^*_L starts to contribute. At Q^2 of the order of $2 \div 3$ GeV^2 σ_L is comparable to σ_T, at higher Q^2 production by γ^*_L predominates.

As mentioned in Sec. 1.4, R provides a sensitive test of theoretical models. Several models are known which have been successful in describing R in a Q^2 range of the COMPASS data, e.g. [3] based on generalized VMD ideas and [18] based on partonic–QCD approach.

In Fig. 5 (left panel) $r^1_{1\,-1}$ SDM element is shown as a function of Q^2. One can notice its decrease with Q^2, which is a direct consequence of a decrease of the amplitude of oscillations of the ψ angle, see Eq. (6). If SCHC holds, and additionally an object with a *natural* parity $P = (-1)^J$ is exchanged in the t-channel of the reaction (2), then SDM elements r^{04}_{00} and $r^1_{1\,-1}$ are related via

$$r^1_{1\,-1} \;=\; \frac{1}{2}\,(1 \;-\; r^{04}_{00})\,. \tag{8}$$

This relation is approximately fulfilled by the results. A precise check of Eq. (8) is foreseen in the forthcoming analysis.

The SDM elements $\mathrm{Im}\, r^3_{1\,-1}$ and $r^{04}_{1\,-1}$, extracted from the ϕ distribution, are shown as a function of Q^2 in Fig. 5 (right panel). $\mathrm{Im}\, r^3_{1\,-1}$ is consistent with zero, as it should be if SCHC holds. In contrast, $r^{04}_{1\,-1}$ in all 5 bins shows a tendency to be negative, $1 \div 2.5$ standard deviations below zero. This indicates a possible weak *violation of SCHC*, and is consistent with the high precision ZEUS results at Q^2 below 1 GeV^2 [15]. The non-zero

value of $r^{04}_{1\,-1}$ indicates a contribution of the helicity-flip amplitude in the γ^*–ρ^0 transition. Further studies will be done to clarify this issue.

The systematic studies concerning the SDM elements included checks of stability of the results over time of data taking, sensitivity of the results to the target polarization, and their dependence on the target cell, in which the primary vertex was reconstructed. No significant effects were observed. The statistical precision of the results is dominated by the limited Monte Carlo sample used for corrections, and not by the 2002 data sample. The non-exclusive background was not subtracted yet, and further studies of it are under way. However, a possible change of the results due to this background effects was estimated to be smaller than the present statistical uncertainties.

After including 2003 and 2004 COMPASS data in the analysis, our sample will contain altogether ~ 6 times more events, which will allow to significantly reduce statistical uncertainties. We plan to determine all 23 ρ^0 SDM elements on a basis of such an extended sample.

5. Summary

The preliminary results for the r^{04}_{00}, $r^{1}_{1\,-1}$, $r^{04}_{1\,-1}$, and $\mathrm{Im}\, r^{3}_{1\,-1}$ ρ^0 meson SDM elements and the ratio R, based on the 2002 COMPASS data, have been presented. They were obtained in the analysis of experimentally determined angular distributions of ρ^0 production and decay, corrected for effects of acceptance, reconstruction efficiency and kinematical smearing. The non-exclusive background has not been subtracted yet. However, its possible effect on the presented results has been estimated to be smaller than the present statistical uncertainties.

COMPASS results are in a good agreement with those of other moderate and high energy experiments. Our precise data allow to extend the Q^2 range investigated in ρ^0 leptoproduction by a decade down with respect to the other experiments. The strong increase of R with Q^2 has been observed. A possible weak violation of the SCHC hypothesis has been noticed, consistent with the earlier result of the ZEUS Collaboration.

The present analysis is planned to be expanded, including 2003 and 2004 COMPASS data. Such a sample will contain ~ 6 times more events than used in the present analysis. This will allow to determine all 23 ρ^0 SDM elements.

The studies of exclusive *coherent* ρ^0 production on the COMPASS nuclear target are planned as well. Another analysis performed at COMPASS is the analysis of the double-spin longitudinal asymmetry of cross sections for exclusive incoherent ρ^0 production. It allows to study spin effects in this reaction when both beam and target are polarized. Studies of exclusive

production of other vector mesons are also planned.

This work was supported in part by KBN SPUB 621/E-78/SPB/CERN/P-03/DWM 576/2003-2006. The author expresses acknowledgements to the organizers for allowing him to present this talk.

REFERENCES

[1] G. Baum et al. (COMPASS Collab.) *COMPASS: A Proposal for a Common Muon and Proton Apparatus for Structure and Spectroscopy*, CERN-SPSLC-96-14, SPSLC-P-297, March 1996.

[2] T.H. Bauer et al., *Rev. Mod. Phys.* **50**, 261 (1978), erratum: ibid. **51**, 407 (1979).

[3] D. Schildknecht, G.A. Schuler, B. Surrow, *Phys. Lett.* **B 449**, 328 (1999).

[4] S.J. Brodsky et al., *Phys. Rev.* **D 50**, 3134 (1994),
L.L. Frankfurt, W. Koepf, M.I. Strikman, *Phys. Rev.* **D 54**, 3194 (1996).

[5] A.D. Martin, M.G. Ryskin, T. Teubner, *Phys. Rev.* **D 55**, 4329 (1997).

[6] M. Diehl *Phys. Rep.* **388**, 41 (2003).

[7] A.D. Martin, M.G. Ryskin, *Phys. Rev.* **D 57**, 6692 (1998).

[8] J.A. Crittenden, *Exclusive production of neutral vector mesons at the electron–proton collider HERA*, Springer-Verlag, Berlin, 1997 (see also `hep-ex/9704009`).

[9] K.P. Schilling, G. Wolf, *Nucl. Phys.* **B 61**, 381 (1973).

[10] G.K. Mallot *Nucl. Instr. Meth.* **A 518**, 121 (2004).

[11] S.D. Drell, *Phys. Rev. Lett.* **5**, 278 (1960).

[12] A. Korzenev, *Exclusive ρ^0 and ϕ production from COMPASS*, in Proc. of the XI Intl. Workshop on Deep Inelastic Scattering *DIS 2003*, St. Petersburg, Russia, 23–27 April 2003, p. 261.

[13] P. Söding, *Phys. Lett.* **19**, 702 (1966).

[14] M.R. Adams et al. (E665 Collab.), *Z. Phys.* **C 74**, 237 (1997).

[15] J. Breitweg et al. (ZEUS Collab.), *Eur. Phys. J.* **C 12**, 393 (2000).

[16] C. Adloff et al. (H1 Collab.), *Eur. Phys. J.* **C 13**, 371 (2000).

[17] M. Derrick et al. (ZEUS Collab.), *Z. Phys.* **C 69**, 39 (1995).

[18] J.R. Cudell, I. Royen, *Phys. Lett.* **B 397**, 317 (1997).